NIH Public Access
Author Manuscript
J Surg Res. Author manuscript; available in PMC 2009 September 1.

Published in final edited form as:
J Surg Res. 2008 September ; 149(1): 47–56. doi:10.1016/j.jss.2007.12.788.

MOLD-SHAPED, NANOFIBER SCAFFOLD-BASED CARTILAGE ENGINEERING USING HUMAN MESENCHYMAL STEM CELLS AND BIOREACTOR

Sasa Janjanin, M.D., M.S.[*,1,2], **Wan-Ju Li, Ph.D.**[*,1], **Meredith T. Morgan, Ph.D.**[1], **Rabie M. Shanti, B.S.**[1,3], and **Rocky S. Tuan, Ph.D.**[1]

1*Cartilage Biology and Orthopaedics Branch, National Institute of Arthritis, and Musculoskeletal and Skin Diseases, National Institutes of Health, Department of Health and Human Services, Bethesda, MD, 20892*

2*Department of Otorhinolaryngology, Head & Neck Surgery, Zagreb Clinical Hospital Center, Kispaticeva 12, 10000 Zagreb, Croatia*

3*Howard Hughes Medical Institute-National Institutes of Health Research Scholars, Program, Bethesda, MD, 20814*

Abstract

Background—Mesenchymal stem cell (MSC)-based tissue engineering is a promising future alternative to autologous cartilage grafting. This study evaluates the potential of using MSCs, seeded into electrospun, biodegradable polymeric nanofibrous scaffolds, to engineer cartilage with defined dimensions and shape, similar to grafts used for subcutaneous implantation in plastic and reconstructive surgery.

Materials and methods—Human bone marrow derived MSCs seeded onto nanofibrous scaffolds and placed in custom-designed molds were cultured for up to 42 days in bioreactors. Chondrogenesis was induced with either transforming growth factor-β1 (TGF-β1) alone or in combination with insulin-like growth factor-I (IGF-I).

Results—Constructs exhibited hyaline cartilage histology with desired thickness and shape as well as favorable tissue integrity and shape retention, suggesting the presence of elastic tissue. Time-dependent increase in cartilage matrix gene expression was seen in both types of culture; at Day 42, TGF-β1/IGF-I treated cultures showed higher collagen type II and aggrecan expression. Both culture conditions showed significant time-dependent increase in sulfated glycosaminoglycan and hydroxyproline contents. TGF-β1/IGF-I treated samples were significantly stiffer; with equilibrium compressive Young's modulus values reaching 17 kPa by Day 42.

Conclusions—The successful *ex vivo* development of geometrically defined cartilaginous construct using customized molding suggests the potential of cell-based cartilage tissue for reconstructive surgery.

Corresponding Author: Dr. Rocky S. Tuan, Chief, Cartilage Biology and Orthopaedics Branch, National Institute of Arthritis and Musculoskeletal and Skin Diseases, National Institutes of Health, Building 50, Room 1523, MSC 8022, Bethesda, MD 20892-8022, Tel: (301) 451-6854, Fax: (301) 435-8017, Email: tuanr@mail.nih.gov.
*These authors contributed equally

Publisher's Disclaimer: This is a PDF file of an unedited manuscript that has been accepted for publication. As a service to our customers we are providing this early version of the manuscript. The manuscript will undergo copyediting, typesetting, and review of the resulting proof before it is published in its final citable form. Please note that during the production process errors may be discovered which could affect the content, and all legal disclaimers that apply to the journal pertain.

NIH-PA Author Manuscript
NIH-PA Author Manuscript
NIH-PA Author Manuscript

NIH-PA Author Manuscript

NIH-PA Author Manuscript

NIH-PA Author Manuscript

Keywords

mesenchymal stem cells; tissue engineering; cartilage; nanofibers; nanofibrous scaffolds; mold; bioreactor; plastic and reconstructive surgery

INTRODUCTION

Cell-based cartilage tissue engineering is a promising, novel, and multidisciplinary approach that utilizes principles of engineering and life sciences to fabricate functional biological substitutes for the repair or replacement of damaged cartilage [1]. The basic underlying principles of tissue engineering involve using a small initial piece of donor tissue as a cell source, isolating and expanding cells from it to a clinically significant cell number, and seeding the cells on scaffolds in order to get a desirable shape of a neotissue, while supporting their growth and/or differentiation by the addition of appropriate bioactive factors. Because of the epidemiological importance and high societal costs of osteoarthritis, cartilage engineering holds tremendous potential in orthopaedic surgery as an alternative to current surgical methods of alloplastic joint replacement. There is also a significant need for cartilage in facial plastic and reconstructive surgery, although in smaller amount as compared to orthopaedics.

The most common need for cartilage in the head and neck area is in the reconstruction of the nose, the ears and tracheal defects, which can be caused either congenitally, or by trauma or surgical resection [2]. Compared to orthopaedic applications, most of the cartilage grafts utilized in facial surgery are implanted subcutaneously, and must exhibit well-defined shape, thickness, and initial mechanical strength. Today, autologous cartilage graft is a gold standard for auricular and nasal reconstruction. However, excision of donor cartilage requires a second surgical procedure, with potential donor site morbidity [3]. Also, given the limited amount of patient cartilage amenable as grafts for reconstructive procedures, tissue-engineering advances represent a significant alternative to current surgical practices.

As a cell source for cartilage tissue engineering, autologous chondrocytes have limited doubling potential, and passaged monolayer cultures dedifferentiate to fibroblasts and cease to produce cartilage ECM molecules [4]. Mesenchymal stem cells (MSCs) are adult tissue-derived multipotent cells with the capacity to differentiate into into cells of osteogenic, chondrogenic, adipogenic and myogenic lineages, and today are considered as a promising cell source for the regeneration of skeletal tissues, owing to ease of isolation, expansion and multipotentiality [5,6].

Chondrogenic differentiation of MSCs requires a three-dimensional environment that serves to enhance cell-cell interactions favorable for chondrogenesis. Our recent studies have shown the utility of electrospun polymeric nanofibrous biomaterials as a biomimetic scaffold for *ex vivo* tissue engineering, because of their morphological similarity to the ECM of the natural environment [7,8] These scaffolds supported the maintenance of chondrocyte phenotype [9] as well chondrogenic induction of MSCs [10], as evidenced by chondrocyte-specific gene expression and synthesis of cartilage ECM.

In this study, we have evaluated the potential application of chondrogenically induced MSCs seeded within electrospun polymeric nanofibrous scaffolds in the *ex vivo* engineering of cartilage grafts, similar to those that are used for subcutaneous implantation in plastic and reconstructive surgery. Such grafts should encompass a tissue-engineered cartilage of significant size, of well-defined dimensions and shape, having thickness resembling either auricular or nasal cartilage, and with desirable biomechanical properties. To obtain desired shape and thickness, we used an external molding system, made from inert, non-adhesive

NIH-PA Author Manuscript

NIH-PA Author Manuscript

NIH-PA Author Manuscript

materials. Packed MSC-nanofiber composites with optimized cell distribution were delivered inside the mold, and incubated in chondrogenic medium supplemented with various growth factors. The molded MSC-nanofiber composites were cultured in spinner flask bioreactors to promote tissue growth via enhancing nutrition transportation and mechanical stimulation.

Our results showed that the procedure resulted in engineered cartilage constructs with defined shape, adequate mechanical properties, and robust expression of chondrogenic phenotype.

MATERIALS AND METHODS

MSC Isolation and Culture

With Institutional Review Board approval, bone marrow-derived MSCs obtained from patients undergoing lower extremity reconstructive surgery were processed [11]. Briefly, bone marrow aspirates were plated overnight in T-150 cm^2 polystyrene cell culture flasks in a basal medium composed of Dulbecco's Modified Eagle's medium (DMEM; BioWhittaker, Walkersville, MD) supplemented with 10% fetal bovine serum (FBS) from selected lots (Gibco BRL, Life Technologies, Grand Island, NY) and antibiotics (50 μg/mL streptomycin, 50 IU/mL of penicillin; Cellgro, Herndon, VA), and maintained at 37°C in a humidified, 5% CO_2 atmosphere. Nonadherent cells were removed from cultures after 24 h by a series of phosphate buffered saline (PBS; Gibco BRL) washes and subsequent medium changes. After that, medium was replaced every 3–4 days. At 80% confluency, as determined by phase contrast microscopy, cells were washed twice with PBS, detached using 0.25% trypsin-EDTA solution (Gibco BRL), washed twice with expansion medium with centrifugation (1,200 rpm for 5 minutes), and replated at 1:3 in triple flasks (Nunc, Roskilde, Denmark) under same culture conditions. All cells were used at passage 3.

Nanofibrous Scaffold Production

Nanofibrous scaffolds were fabricated by electrospinning as described previously [12]. Briefly, poly(L-lactic acid) (PLLA; Polysciences, Warrington, PA) in chloroform/dimethyformamide (10:1) was electrospun to produce a homogeneous mat of approximately 1.5 mm thickness. After solvent removal and desiccation, the PLLA mat was cut into 1 × 1 cm^2 shapes and sterilized by ultraviolet irradiation. The scaffolds were pre-wetted by immersion in Hank's Balanced Salt Solution (HBSS) for 24 h at 37°C.

MSC Seeding on Nanofiber Scaffolds, and Construct Culture and Differentiation

Passage 3 MSCs were seeded at a density of 5×10^6 cells/scaffold onto the surface of pre-wetted scaffolds and placed in 50 ml polypropylene tubes. The tubes were gently vortexed for 10 minutes and then incubated in basal medium at 37°C for 24 h to allow MSCs to diffuse into and adhere to the scaffold. After 24 hours, cellular scaffolds were transferred under sterile conditions into custom-designed molds (Figure 1). The mold consisted of two separate polypropylene halves, with a silicone washer to define the dimensions and thickness of the engineered tissue constructs (10×10×2 mm). The polypropylene halves were tightly secured with small polypropylene screws at one side of the mold, and with stainless steel screws at the other side of the mold. Because of the unequal weight between the stainless steel screws and the polypropylene screws, this design allowed the molds containing cellular scaffolds to suspend vertically in the bioreactor and to be accessible for nutrient diffusion from both sides of the mold via numerous perforating holes of 1 mm diameter located in both polypropylene halves.

Once encased in molds, cellular constructs were transferred into spinner flasks (Bellco Biotechnology, Inc., NJ, USA) and cultured under chondrogenic conditions at a mixing rate of 30 rpm (Figure 2). Chondrogenic medium (500 mL in each spinner flask) consisted of high-

NIH-PA Author Manuscript

NIH-PA Author Manuscript

NIH-PA Author Manuscript

glucose DMEM, supplemented with 100 nM dexamethasone (Sigma-Aldrich, St. Louis, MO), 50 μg/mL ascorbic acid-2-phosphate (Sigma-Aldrich), 100 μg/mL sodium pyruvate (Sigma-Aldrich), 40 μg/mL L-proline (Sigma-Aldrich), 50 mg/mL ITS-premix stock (BD Biosciences, San Jose, CA), and 50 U/mL penicillin and 50 μg/mL streptomycin. Cells were induced to undergo chondrogenesis in two different growth factor conditions: (1) chondrogenic medium supplemented with 10 ng/mL recombinant human transforming growth factor-β1 (TGF-β1; R&D Systems, Minneapolis, MN), and (2) chondrogenic medium supplemented with both 10 ng/mL TGF-β1 and 100 ng/mL of insulin-like growth factor-I (IGF-I; R&D Systems). Medium changes were carried out twice weekly.

Samples were harvested after 14, 28 and 42 days under sterile conditions, and used for real-time RT PCR determination of mRNA profile, biochemical analyses, histology and biomechanical testing.

RNA isolation and real-time RT-PCR analysis

Constructs harvested at each time point were extracted for total cellular RNA using Trizol Reagent (Gibco BRL) according to the manufacturer's protocol. For efficient yield, constructs were homogenized for 15 minutes in Trizol Reagent using a pestle (Kontes, Vineland, NJ). RNA concentrations were estimated spectrophotometrically on the basis of A_{260}. RNA samples were reverse transcribed using random hexamers and the SuperScript First Strand Synthesis System (Gibco BRL). Gene expression analysis was detected using iQ SYBR Green supermix in the Bio-Rad iCycler iQ system [13]. Gene-specific oligonucleotide primers included collagen type II (COL2A1), aggrecan, collagen type I (COL1A1), elastin, and glyceraldehyde-3-phosphate dehydrogenase (G3PDH) as an internal control for mRNA loading. Relative expression levels for the lineage specific genes were calculated using standard curves generated from triplicated dilution series of cDNA and normalized to the housekeeping gene, G3PDH.

Sulfated glycosaminoglycan (sGAG) assay

Commercially available sGAG assay kit (Blyscan; Biocolor Ltd, Newtownabbey, Northern Ireland) was used. sGAGs were extracted using papain digestion [14], and incubated with the Blyscan dye reagent, 1, 9-dimethylmethylene blue. Bound dye released from the insoluble sGAG-dye complex was quantified spectrophotometrically (A_{656}), and sGAG content estimated using chondroitin 4-sulfate as a standard.

Cell proliferation assay

Extracts derived from the GAG assay described above was used to estimate cell number based on DNA assay using the RediPlatet 96 PicoGreen dsDNA Assay (Invitrogen, Carlsbad, CA). The PicoGreen–DNA complex was detected fluorimetrically (excitation/emission at 490/520 nm) using a multiwell plate reader (Synergy HT, BioTek, Highland Park, VT), and DNA content estimated using a commercial standard.

Collagen content analysis

Samples were analyzed for hydroxyproline contents as an estimate of collagen level as described previously [15]. Briefly, papain digests were hydrolyzed with equal volumes of 4N KOH at 120°C for 30 minutes. Chloramine-T and Ehrlich's reagent were added to the hydrolysates and A_{560} determined using a multiwell plate reader. Hydroxyproline content was expressed as ng/μg DNA.

NIH-PA Author Manuscript

NIH-PA Author Manuscript

NIH-PA Author Manuscript

Histology

Cellular constructs were washed in PBS, fixed in 4% phosphate-buffered paraformaldehyde at 4°C for 30 min, dehydrated through a graded series of ethanol, infiltrated with HistoClear (National Diagnostics, Atlanta, GA), embedded in paraffin, and sectioned at 8 μm thickness. For histological analysis, sections were rehydrated and stained with hematoxylin and eosin (H&E) and Alcian blue (pH 1.0).

Biomechanical testing

Mechanical testing was performed as described previously using a custom apparatus [16]. Sample thickness and dimensions were measured with a digital micrometer. Constructs were tested in unconfined compression between two smooth impermeable surfaces in PBS at room temperature. Samples were first tested for 300 s in creep under a tare load of 0.02 N applied until equilibrium was achieved. Subsequently, stress relaxation tests were carried out with a compressive deformation of 1 μm/s to 10%, after which samples were allowed to relax to equilibrium (1200 s). The equilibrium compressive Young's modulus was determined from the equilibrium force normalized to the original cross-sectional area divided by the equilibrium compressive strain.

Statistical analysis

Data were expressed as mean ± standard deviation (SD) and analyzed statistically using Two-Way ANOVA in Microsoft Excel 2004 for Mac, version 11.2 (Microsoft Corporation, Redmond, WA), with significance set at $p \leq 0.05$.

RESULTS

Gross morphology

After 14, 28 and 42 days of culture, the constructs were carefully removed from molds and examined for gross morphological features, including external size, shape, structural details, and texture of the tissue to palpation. All the molds were able to generate tissue with the desired thickness and shape (Figure 3). The MSC-based cartilage constructs exhibited favorable tissue integrity, were capable of restoring shape after bending and warping between fingers, and moderate pinching and stabbing with a forceps tip, as well as retaining position when placed vertically, suggesting the presence of elastic, biological tissue. The surface of the constructs was glossy, but somewhat irregular, because of small protrusions of neotissue formed through the perforations created in the mold for nutrient transport. The internal dimensions of the molds used were 10×10×2 mm, while the measured length, width and height of harvested constructs (mm) were: 9.32±0.68, 8.96±0.75 and 2.05±0.03 (Day 14); 9.02±1.29, 9.25±0.87 and 1.99 ±0.02 (Day 28), and 8.86±0.59, 9.18±0.83 and 1.98±0.02 (Day 42), respectively.

Expression of cartilage-specific genes

Real-time RT-PCR analysis was used to analyze the mRNA expression of cartilage-specific genes from MSCs cultured in the two growth factor conditions: (1) chondrogenic medium supplemented with TGF-β1, and (2) chondrogenic medium supplemented with both TGF-β1 and IGF-I. Constructs from both conditions showed significant change in cartilage-specific gene expression over time (Figure 4). After 42 days in the culture, the mRNA levels of aggrecan (Figure 4A) and collagen type II (Figure 4B) in TGF-β1/IGF-I treated cultures were notably higher than those treated only with TGF-β1, although differences in mRNA expression between growth factor groups were not statistically significant. Both TGF-β1 and TGF-β1/IGF-I treated samples showed comparable mRNA levels of collagen type I (Figure 4C) and elastin (Figure 4D). At Day 14, collagen type II/collagen type I ratio showed no difference between groups, but after 42 days it was 0.32 for TGF-β1 treated group, and 1.40 for TGF-β1/IGF-I group

NIH-PA Author Manuscript

NIH-PA Author Manuscript

NIH-PA Author Manuscript

(Student's T-test, Microsoft Excel 2004; $p<0.05$). The increase in collagen type II/collagen type I ratio indicated progress towards more mature cartilage phenotype over time, and the medium supplemented with both TGF-β1 and IGF-I was therefore considered a more favorable condition for chondrogenic differentiation of MSCs seeded in nanofibrous scaffold.

Biochemical analysis

DNA content was measured to quantify the cell density of tissue-engineered cartilage constructs. The DNA content of samples was very constant, and did not show significant increase over time points. Also, there was no significant difference in DNA content between the two growth factor conditions (Figure 5). The average content of DNA per single construct was 108.74±33.96 μg (initial seeding density was 5×10^6 cells per scaffold).

ECM synthesis in the constructs was monitored by measuring the amount of sGAG and hydroxyproline in each sample. In both growth factor condition groups, the amount of ECM increased with time. In TGF-β1 groups, sGAG/DNA increased from 16.90±8.97 μg/μg to 38.98 ±22.71 μg/μg, while in TGF-β1/IGF-I treated groups it increased from 21.84±17.76 μg/μg to 44.90±16.70 μg/μg, for culture Days 14 and Days 42, respectively (Figure 6). Hydroxyproline content also gradually increased with time in both growth factor conditions: between Day 14 and Day 42, the TGF-β1 treated group increased from 5.45±1.47 ng/μg DNA to 11.76±3.02 ng/μg, while the TGF-β1/IGF-I treated samples increased from 4.78±1.74 ng/μg to 14.38±2.90 ng/μg (Figure 7). Overall, in both TGF-β1 and TGF-β1/IGF-I treated groups, both sGAG and hydroxyproline accumulation showed significant changes over culture time ($p<0.01$ for sGAG, $p<0.001$ for hydroxyproline). Also, for all time points, no significant difference in sGAG and hydroxyproline contents was observed between the two medium conditions.

Mechanical properties

The equilibrium mechanical properties of the MSC/nanofiber constructs improved as a function of culture time ($p<0.001$), and they were also depended on growth factor condition ($p<0.05$). The equilibrium Young's modulus of the TGF-β1 treated constructs increased from 3.15±0.46 kPa on Day 14 to 12.17±2.54 kPa on Day 42. TGF-β1/IGF-I treated samples had similar values to TGF-β1 group at the first two time points (3.26±0.45 kPa and 9.8±2.14 kPa, respectively), but were significantly stiffer by Day 42, reaching 16.96±2.45 kPa (Figure 8).

Histology

H&E staining revealed that, at early time points (Days 14 and 28), the tissue constructs showed areas of both high and low cellularity, and there was no observable difference between superficial and inner regions. By Day 42, cells assumed a more rounded shape, and showed cellular distribution resembling the distribution of chondrocytes in native cartilage (Figure 9 A–F). Although a dense superficial layer of cells was apparent in some constructs, there was no formation of fibrous capsule. Cellular density and distribution appeared similar in constructs maintained under the two growth factor conditions, for both internal and surface regions.

Alcian blue staining increased in intensity and area as a function of culture time in both culture conditions, demonstrating the production of sulfated proteoglycan-rich ECM, typical of cartilage (Figure 9 G–L). On Day 14, only weak, uniform staining was observed throughout the constructs, in both sections through the edge as well as through the center. By Day 42, increased staining was seen, consistent with the accumulation of cartilaginous ECM, particularly in the IGF-I/TGF-β1 treated group; in both groups, sections through the edges of constructs stained better than those sectioned through the central core (Figure 9 M, N).

NIH-PA Author Manuscript

NIH-PA Author Manuscript

NIH-PA Author Manuscript

DISCUSSION

In this study, we have evaluated the potential of using adult human bone marrow-derived MSCs and electrospun polymeric nanofibrous scaffolds to engineer cartilage grafts of pre-defined dimensions and shape, similar to grafts harvested from autologous cartilage and currently used in plastic and reconstructive surgical procedures. For subcutaneous implantation applications (especially when cartilage grafts are implanted underneath thin, sensitive skin such as that in the ear or the nose), tissue engineered cartilage grafts should offer aesthetic results equal or even superior to current techniques of autologous cartilage grafting, as even small irregularities can be visible or palpable and produce unfavorable results.

There have been recent reported attempts in the engineering of shaped cartilage constructs. Alhadlaq et al. [17] described the use of photopolymerized polyurethane mold to shape cell/biocompatible polymer suspension. Hott et al. [18] used computer-aided design and injection molding technologies to fabricate small, precisely shaped chondrocyte-seeded calcium alginate structures in the shape of butterfly tympanic membrane patches. Neumeister et al. [19] used silicone mold placed over transposed vessels in the abdominal wound pocket of the rat to form and shape vascularized molded fibrous capsule, which was later filled with chondrocytes and a fibrin glue carrier. Kamil at al. reported the *in vivo* use of extrinsic molding system in providing shape, size, and biomechanics of the tissue-engineered cartilage construct. A perforated, auricle shaped hollow gold mold was filled with mixtures of autogenous chondrocytes and biodegradable polymers, and implanted subcutaneously in the abdominal area of pigs and sheep over 8 to 20 weeks [20]. The implants resulted in cartilage with essentially normal histology, although leakage outside the molds and external cartilage generation was noted.

In this study, to generate tissue-engineered cartilage with pre-determined shape, size and thickness, we have designed polypropylene molds, with pores that allowed medium/nutrient access, to culture MSCs seeded within three-dimensional nanofibrous polymeric scaffolds and induced to undergo chondrogenesis. The molds used were of a dimension of 10×10×2 mm. Engineered neotissue precisely maintained the desired shape and pre-defined dimensions during in vitro culture, throughout all time points. Furthermore, even as early as culture Day 14, the MSC-generated tissue exhibited favorable integrity, and although softer than native cartilage, exhibited observable shape memory after physical deformation (bending and warping between fingers as well as pinching with forceps), and was able to retain position when placed vertically. The surface of all constructs was white and glossy, but somewhat irregular, because of minor leakage of neotissue through the feed pores of the mold.

A tissue-engineered scaffold serves as a three-dimensional biomaterial matrix, that acts as a replacement of the natural extracellular matrix until the seeded cells can produce a new natural matrix and regenerate desired tissue structure. Critical parameters for tissue engineering scaffold include biocompatibility, biodegradability, optimal mechanical strength, and ability to regulate appropriate cellular activities. Biodegradable polymers are currently being actively tested for tissue engineering applications and, ideally, optimal tissue regeneration should occur upon complete biodegradation of the polymeric matrix followed by restoration of biological functions.

Poly(α-hydroxy esters) are the most commonly used synthetic polymers in tissue engineering applications. Recently, to critically assess the applicability of the electrospinning technology for scaffold fabrication, we electrospun and characterized six commonly used poly(alpha-hydroxy esters) [10]. Our findings showed that PLLA- and PCL-based fibrous scaffolds exhibited the most favorable physical and biological characteristics, such as the maintenance of scaffold structure in physiological buffer and the support of cell proliferation, making them

NIH-PA Author Manuscript

NIH-PA Author Manuscript

NIH-PA Author Manuscript

promising for the engineering of more structurally stable connective tissues. In addition, PLLA scaffolds supported the highest rate of proliferation of seeded chondrocytes and MSCs compared to other polymeric scaffolds, the reason for our choice of PLLA scaffolds in this study.

The cultures were incubated in spinner flask bioreactors to maximize nutrient transfer to the engineered tissue construct through the perforations in the mold. While spinner cultures have been favored over static cultures because of continuous flow of medium [21], the turbulent flow and associated higher shear stress generated within the spinner flasks are generally considered their main disadvantages. Some previous studies reported the formation of an outer fibrous capsule in the cartilaginous tissue grown in regular spinner flasks [22]. In the culture design used here, the developing tissue construct was encased in the custom-designed mold and was largely protected from turbulence and direct shear stress, and histological analysis did not reveal such fibrous layer on the surface of the constructs.

Members of the TGF-β superfamily [23] and IGF-I have been shown to be critical for the induction of chondrogenic differentiation of MSCs, with some studies showing a synergistic role for IGF-I and TGF-β1 in maintaining the matrix [24]. In a previous study, we observed that both a three-dimensional environment and TGF-β1 are necessary for successful chondrogenesis. In the absence of TGF-β1 treatment, no cartilage-like layer formed in either cartilage pellet or nanofibrous scaffold cultures. In contrast, TGF-β1 supplemented cultures showed round cells with chondrocyte-like morphology [10]. Our results reported here further support the use of either TGF-β1, or a combination of IGF-I and TGF-β1, for *in vitro* cartilage tissue engineering, in terms of enhanced aggrecan, collagen, and sGAG production over time. In addition, in TGF-β1/ IGF-I treated cultures we observed a significant increase in the ratio of collagen type II to collagen type I over time, consistent with progress towards a cartilaginous phenotype. The collagen type II/collagen type I mRNA ratio was also significantly different between the two growth factor conditions after 42 days in culture (0.32 and 1.40, for TGF-β1 alone and TGF-β1/IGF-I combination, respectively; $p<0.05$). However, since changes in mRNA levels may not always correlate directly with protein levels, Western blot analysis is needed to ascertain differences in the level of collagen types I and II, as well as other proteins of interest.

Mechanical testing showed that the TGF-β1/IGF-I combination yielded tissue constructs with higher mechanical properties. While the equilibrium Young's modulus of MSC-nanofibrous scaffold constructs increased with time in both culture groups, the values were significantly higher in the TGF-β1/IGF-I group ($p<0.05$), reaching 16.96±2.45 kPa by Day 42. This change of mechanical properties was somewhat surprising as IGF-I addition does not significantly affect DNA, sGAG and hydroxyproline contents and aggrecan expression between the two groups. Some studies have shown that IGF-I reduces the expression and secretion of collagenase enzymes, as well as downregulates matrix metalloproteinase (MMP) mRNA expression (MMP-1, MMP-3, MMP-8, and MMP-13) [25]. Therefore, we speculate that differences in biomechanical properties between the two growth factor groups could be related to different activity of cartilage breakdown enzymes that had impact on the retention and stability of matrix components.

It is noteworthy that the values of the equilibrium Young's modulus were still significantly lower than that of native cartilage or chondrocyte-based tissue engineered constructs [26]. Recent data from our laboratory [**Li and Tuan**, unpublished] showed that cell-nanofiber composites derived from primary bovine chondrocytes are able to reach an equilibrium Young's modulus of 120 kPa by culture Day 42. These results suggest that while MSC-laden scaffolds can develop molecular and biochemical properties of cartilage, MSCs are significantly less able to develop a mechanically functional matrix, compared to fully differentiated

NIH-PA Author Manuscript

NIH-PA Author Manuscript

NIH-PA Author Manuscript

chondrocytes. Thus, our mold-based model to engineer cartilage of desired shape will require further optimization, to ensure that MSC chondrogenic differentiation and ECM synthesis are maximally promoted.

Other studies that used MSCs as a cell source for cartilage tissue engineering have reported similar observations. Mechanical properties of adipose-derived MSC-laden hydrogels suggest that while the cells undergo chondrogenic differentiation, the constructs did not acquire significant material properties over a 4-week culture period [27]. Mauck et al. showed that bovine MSCs seeded in agarose and cultured under chondrogenic conditions showed significant accumulations of cartilaginous ECM, but the mechanical properties achieved in these gels were two- to three-fold lower than that produced by chondrocytes isolated from the same animals and cultured under the same conditions [28]. On the other hand, Park et al. analyzed mechanical properties of chondrocyte-based engineered cartilage, and found the neo-cartilage similar to native cartilage in all three mechanical parameters measured - ultimate tensile strength, stiffness, and resilience [29]. These findings that MSCs, even cultured under “optimal” chondrogenic conditions, still under-perform when compared to primary chondrocytes, indicate the importance of prior history of cells in cell-based cartilage engineering as well as the specific requirements of optimal mesenchymal chondrogenesis *in vitro*. In addition, it also remains to be established as to what percentage of MSCs isolated using the conventional methods possess chondrogenic potential, i.e., the ability to differentiate into mature chondrocytes and subsequently produce a functional and mechanically stable cartilaginous ECM [30].

In summary, our results strongly suggest that a molding system can be successfully used for *in vitro* pre-shaping of MSC-based tissue engineered cartilage constructs. The nanofibrous scaffold used here proved to be a highly functional biomaterial matrix, supporting homogeneous cell distribution, efficient cell differentiation, and ECM expression, production and assembly, as shown by histology, and real-time RT-PCR and biochemical analyses. MSCs are currently considered an attractive cell source in regenerative medicine, due to their simplicity of isolation and high expansion potential. *Ex vivo* culture expansion of allogeneic donor MSCs can result in over 10,000-fold increase in the number of MSCs when compared to unmanipulated bone marrow transplantation [31]. Thus, less than 0.5 ml of bone marrow aspirate is needed to yield the five million cells used in our experiment to form a single 10×10×2 mm piece of cartilage. Taken together with the ability of the molding system to generate shape and form, the production of MSC-based engineered cartilage suitable for subcutaneous grafting applications in plastic and reconstructive surgery should be feasible, provided optimization factors and conditions are established to achieve fully functional chondrogenic differentiation of MSCs.

Acknowledgment

This work is supported by the Intramural Research Program of NIAMS, NIH (ZO1 41131). Sasa Janjanin is a recipient of the Fulbright Scholarship of the U.S. Department of State.

LITERATURE

1. Kuo CK, Li WJ, Mauck RL, Tuan RS. Cartilage tissue engineering: its potential and uses. Curr Opin Rheumatol 2006;18:64. [PubMed: 16344621]
2. Rotter N, Haisch A, Bucheler M. Cartilage and bone tissue engineering for reconstructive head and neck surgery. Eur Arch Otorhinolaryngol 2005;262:539. [PubMed: 16091977]
3. Ohara K, Nakamura K, Ohta E. Chest wall deformitiesand thoracic scoliosis after costal cartilage graft harvesting. Plast Reconstr Surg 1997;99:1030. [PubMed: 9091899]

NIH-PA Author Manuscript

NIH-PA Author Manuscript

NIH-PA Author Manuscript

4. Mayne R, Vail M, Mayne PM, Miller EJ. Changes in the type of collagen synthesized as clones of chick chondrocytes grow and eventually lose division capacity. Proc Natl Acad Sci USA 1976;73:1674. [PubMed: 1064040]
5. Pittenger MF, Mackay AM, Beck SC, Jaiswal RK, Douglas R, Mosca JD, Moorman MA, Simonetti DW, Craig S, Marshak DR. Multilineage potential of adult human mesenchymal stem cells. Science 1999;284:143. [PubMed: 10102814]
6. Chen FH, Rousche KT, Tuan RS. Technology Insight: adult stem cells in cartilage regeneration and tissue engineering. Nat Clin Pract Rheumatol 2006;2:373. [PubMed: 16932723]
7. Li WJ, Laurencin CT, Caterson EJ, Tuan RS, Ko FK. Electrospun nanofibrous structure: a novel scaffold for tissue engineering. J Biomed Mater Res 2002;60:613. [PubMed: 11948520]
8. Li WJ, Mauck RL, Tuan RS. Application of nanofibrous scaffolds in skeletal tissue engineering. J Biomed Nanotechnol 2005;1:1.
9. Li WJ, Danielson KG, Alexander PG, Tuan RS. Biological response of chondrocytes cultured in three-dimensional nanofibrous poly(ε-caprolactone) scaffolds. J Biomed Mater Res 2003;A 67:1105.
10. Li WJ, Tuli R, Okafor C, Derfoul A, Danielson KG, Hall DJ, Tuan RS. A three-dimensional nanofibrous scaffold for cartilage tissue engineering using human mesenchymal stem cells. Biomaterials 2005;26:599. [PubMed: 15282138]
11. Tuli R, Nandi S, Li WJ, Tuli S, Huang X, Manner PA, Laquerriere P, Noth U, Hall DJ, Tuan RS. Human mesenchymal progenitor cell-based tissue engineering of a single-unit osteochondral construct. Tissue Eng 2004;10:1169. [PubMed: 15363173]
12. Li WJ, Cooper JA Jr, Mauck RL, Tuan RS. Fabrication and characterization of six electrospun poly (alpha-hydroxy ester)-based fibrous scaffolds for tissue engineering applications. Acta Biomater 2006;2:377. [PubMed: 16765878]
13. Wang X, Manner PA, Horner A, Shum L, Tuan RS, Nuckolls GH. Regulation of MMP-13 expression by RUNX2 and FGF2 in osteoarthritic cartilage. Osteoarthritis Cartilage 2004;12:963. [PubMed: 15564063]
14. Farndale RW, Buttle DJ, Barrett AJ. Improved quantitation and discrimination of sulphated glycosaminoglycans by use of dimethylmethylene blue. Biochim Biophys Acta 1986;883:173. [PubMed: 3091074]
15. Reddy GK, Enwemeka CS. A simplified method for the analysis of hydroxyproline in biological tissues. Clin Biochem 1996;29:225. [PubMed: 8740508]
16. Mauck RL, Soltz MA, Wang CC, Wong DD, Chao PH, Valhmu WB, Hung CT, Ateshian GA. Functional tissue engineering of articular cartilage through dynamic loading of chondrocyte-seeded agarose gels. J Biomech Eng 2000;122:252. [PubMed: 10923293]
17. Alhadlaq A, Mao JJ. Tissue-engineered neogenesis of human-shaped mandibular condyle from rat mesenchymal stem cells. J Dent Res 2003;82:951. [PubMed: 14630893]
18. Hott ME, Megerian CA, Beane R, Bonassar LJ. Fabrication of tissue engineered tympanic membrane patches using computer-aided design and injection molding. Laryngoscope 2004;114:1290. [PubMed: 15235363]
19. Neumeister MW, Wu T, Chambers C. Vascularized tissue-engineered ears. Plast Reconstr Surg 2006;117:116. [PubMed: 16404257]
20. Kamil SH, Vacanti MP, Aminuddin BS, Jackson MJ, Vacanti CA, Eavey RD. Tissue engineering of a human sized and shaped auricle using a mold. Laryngoscope 2004;114:867. [PubMed: 15126746]
21. Gooch KJ, Kwon JH, Blunk T, Langer R, Freed LE, Vunjak-Novakovic G. Effects of mixing intensity on tissue-engineered cartilage. Biotechnol Bioeng 2001;72:402. [PubMed: 11180060]
22. Freed LE, Vunjak-Novakovic G. Cultivation of cellpolymer tissue constructs in simulated microgravity. Biotechnol Bioeng 1995;46:306. [PubMed: 18623317]
23. Johnstone B, Hering TM, Caplan AI, Goldberg VM, Yoo JU. In vitro chondrogenesis of bone marrow-derived mesenchymal progenitor cells. Exp Cell Res 1998;238:265. [PubMed: 9457080]
24. Sakimura K, Matsumoto T, Miyamoto C, Osaki M, Shindo H. Effects of insulin-like growth factor I on transforming growth factor beta1 induced chondrogenesis of synovium-derived mesenchymal stem cells cultured in a polyglycolic acid scaffold. Cells Tissues Organs 2006;183:55. [PubMed: 17053321]

NIH-PA Author Manuscript

NIH-PA Author Manuscript

NIH-PA Author Manuscript

25. Hui W, Rowan AD, Cawston T. Insulin-like growth factor 1 blocks collagen release and down regulates matrix metalloproteinase-1, -3, -8, and -13 mRNA expression in bovine nasal cartilage stimulated with oncostatin M in combination with interleukin 1alpha. Ann Rheum Dis 2001;60:254. [PubMed: 11171688]

26. Richmon JD, Sage A, Van Wong W, Chen AC, Sah RL, Watston D. Compressive biomechanical properties of human nasal septal cartilage. Am J Rhinol 2006;20:496. [PubMed: 17063745]

27. Awad HA, Wickham MQ, Leddy HA, Gimble JM, Guilak F. Chondrogenic differentiation of adipose-derived adult stem cells in agarose, alginate, and gelatin scaffolds. Biomaterials 2004;25:3211. [PubMed: 14980416]

28. Mauck RL, Yuan X, Tuan RS. Chondrogenic differentiation and functional maturation of bovine mesenchymal stem cells in long-term agarose culture. Osteoarthritis Cartilage 2006;14:179. [PubMed: 16257243]

29. Park SS, Jin HR, Chi DH, Taylor RS. Characteristics of tissue-engineered cartilage from human auricular chondrocytes. Biomaterials 2004;25:2363. [PubMed: 14741601]

30. Javazon EH, Beggs KJ, Flake AW. Mesenchymal stem cells: paradoxes of passaging. Exp Hematol 2004;32:414. [PubMed: 15145209]

31. Koc ON, Day J, Nieder M, Gerson SL, Lazarus HM, Krivit W. Allogeneic mesenchymal stem cell infusion for treatment of metachromatic leukodystrophy (MLD) and Hurler syndrome (MPS-IH). Bone Marrow Transplant 2002;30:215. [PubMed: 12203137]

NIH-PA Author Manuscript
NIH-PA Author Manuscript
NIH-PA Author Manuscript

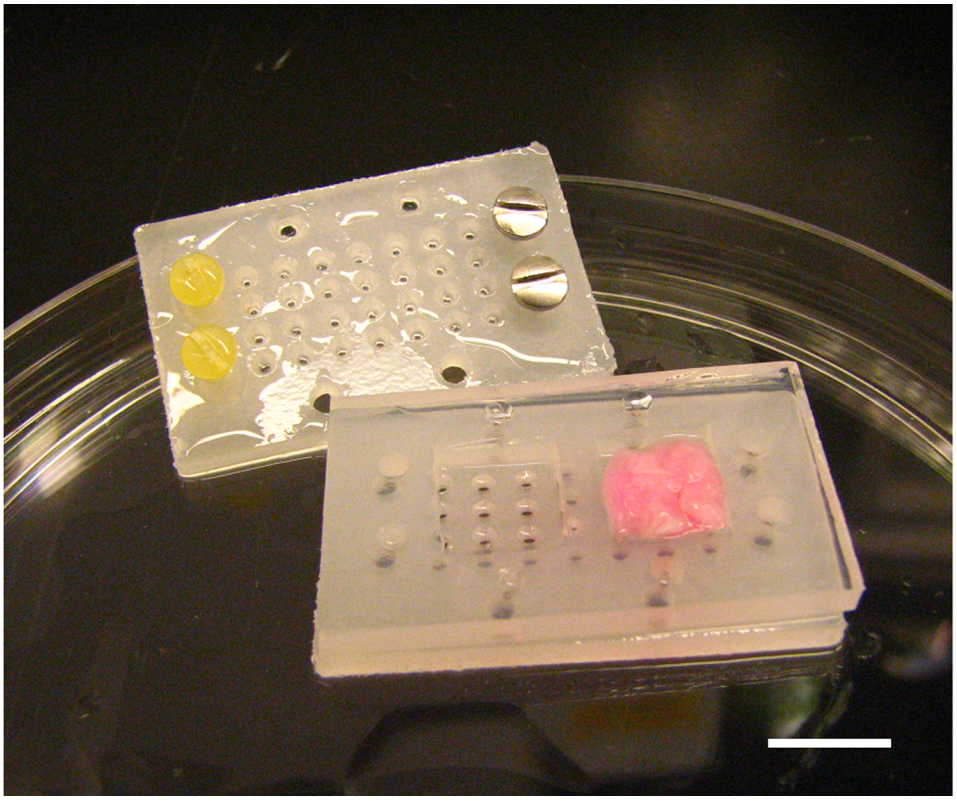

Figure 1.
Custom designed polypropylene molds with silicone sheet that defined dimensions and the shape of the tissue engineered tissue. One mold was designed to produce two pieces of tissue; each with dimensions of 10×10×2 mm. MSC-loaded nanofibrous scaffold can be visualized in the right chamber of the mold. Bar = 10 mm.

NIH-PA Author Manuscript

NIH-PA Author Manuscript

NIH-PA Author Manuscript

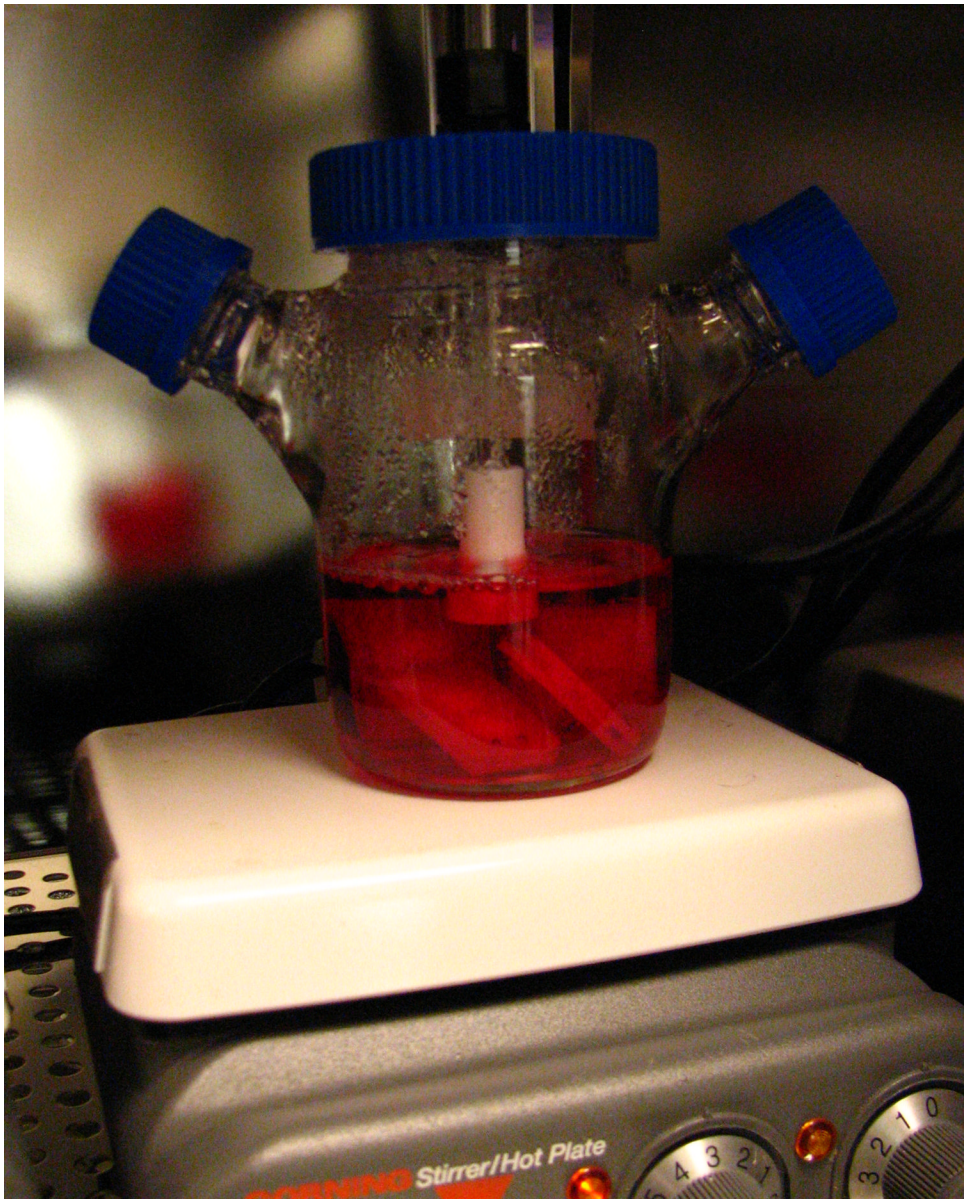

Figure 2.
Spinner flask bioreactor culture system. Molds containing MSC-nanofiber composites are placed into the spinner flask, and maintained in a vertically suspended position due to the placement of stainless steel screws on one end (heavy) and polypropylene screws on the other end (light) of the mold. MSC-nanofiber constructs were cultured under chondrogenic conditions with addition of growth factors for 14, 28 and 42 Days.

NIH-PA Author Manuscript

NIH-PA Author Manuscript

NIH-PA Author Manuscript

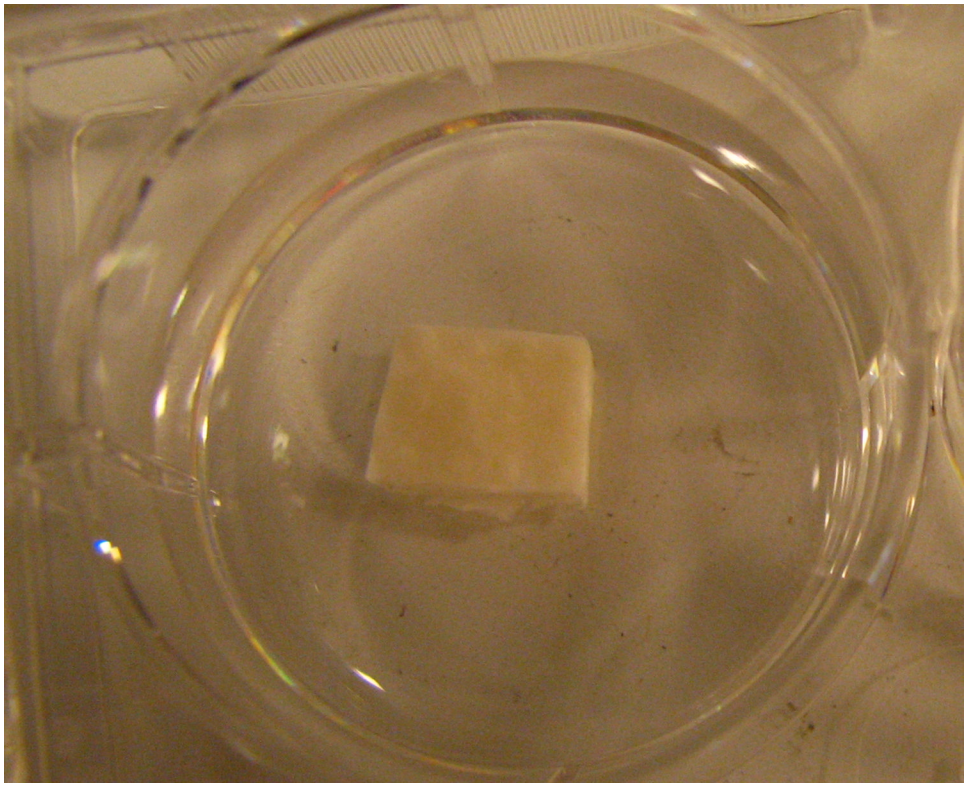

Figure 3.
Cartilaginous construct after 42 days in culture. Constructs were glossy in appearance, white, and resistant to physical deformation.

NIH-PA Author Manuscript
NIH-PA Author Manuscript
NIH-PA Author Manuscript

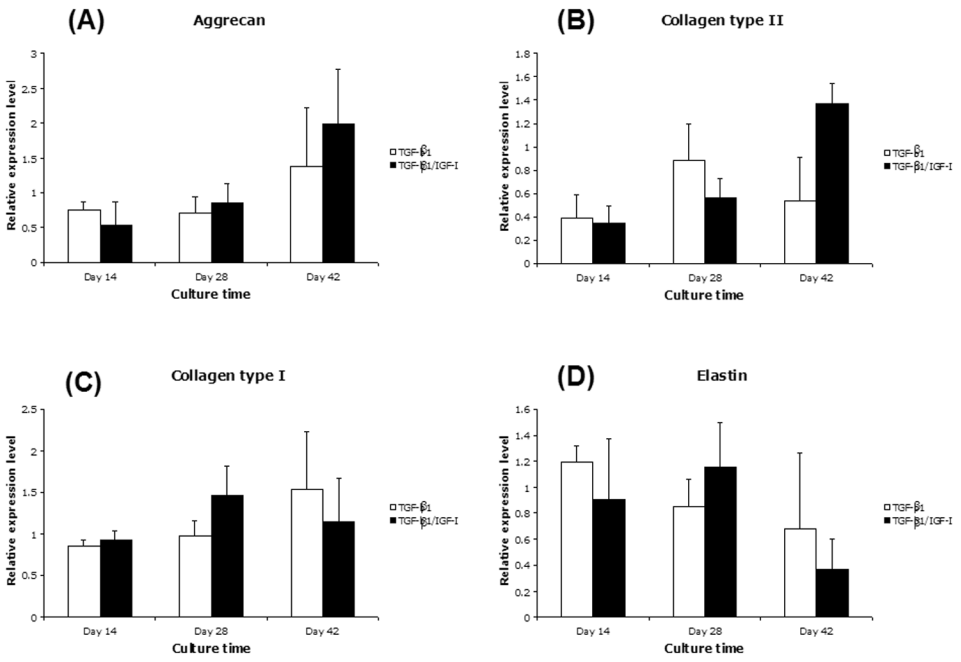

Figure 4.

Cartilage matrix gene expression in engineered cartilage constructs analyzed by real-time, quantitative RT-PCR after Days 14, 28 and 42, respectively. MSC-nanofiber constructs were cultured in chondrogenic medium containing TGF-β1 alone or TGF-β1/IGF-I. Gene expression was analyzed by real-time RT-PCR for (A) aggrecan, (B) collagen type II, (C) collagen type I, and (D) elastin. mRNA values of each gene were normalized to those of the housekeeping gene, G3PDH. All values were mean ± SD. Data were analyzed using two-way ANOVA. Aggrecan, collagen type II, collagen type I, and elastin gene expression changed as a function of culture time ($p<0.001$ for aggrecan and collagen type II, $p<0.05$ for collagen type I, $p<0.005$ for elastin). Compared to TGF-β1 cultures, TGF-β1/IGF-I cultures did not show significant change of levels of mRNA expression of any of these markers ($p>0.05$).

NIH-PA Author Manuscript
NIH-PA Author Manuscript
NIH-PA Author Manuscript

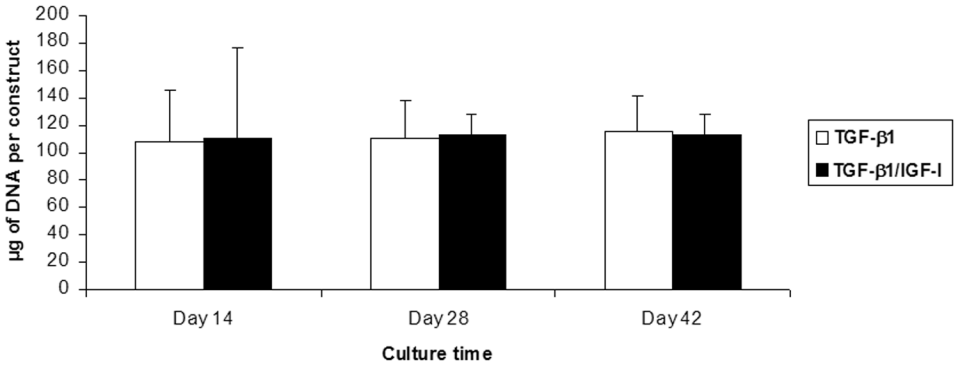

Figure 5.

DNA content of engineered cartilage constructs as a function of culture time. DNA content remained constant, and did not show significant increase over time or between the two growth factor culture conditions (TGF-β1 *vs.* TGF-β1/IGF-I; $p>0.05$). The average DNA content per single construct was 108.74±33.96 µg.

NIH-PA Author Manuscript

NIH-PA Author Manuscript

NIH-PA Author Manuscript

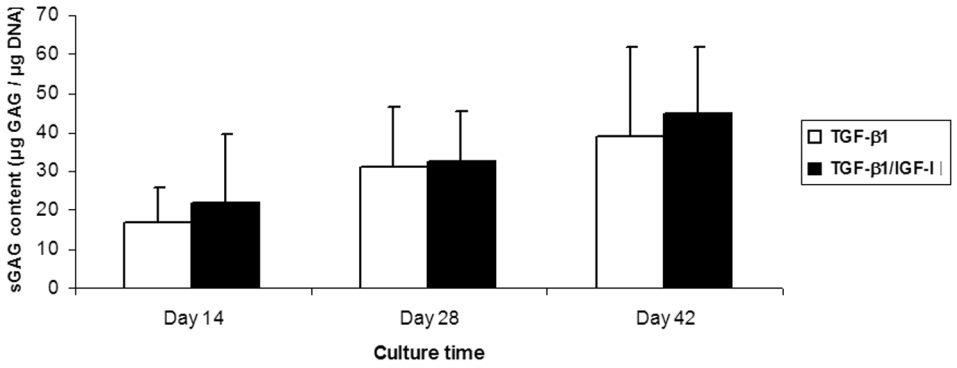

Figure 6.

sGAG content of engineered cartilage constructs as a function of culture time and conditions. In both culture groups (TGF-β1 and TGF-β1/IGF-I), the amount of matrix sGAG changed significantly with time ($p<0.01$). There was no statistically significant difference in sGAG levels between the two growth factor conditions ($p>0.05$). Values are mean ± SD ($n=6$).

NIH-PA Author Manuscript
NIH-PA Author Manuscript
NIH-PA Author Manuscript

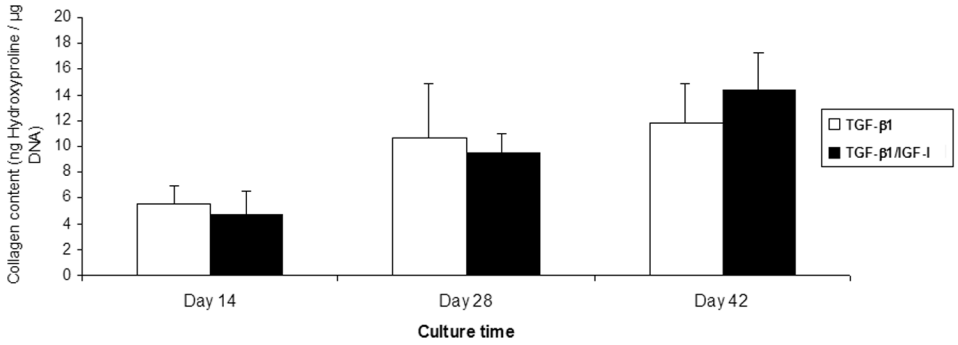

Figure 7.

Collagen level in engineered cartilage constructs, estimated based on hydroxyproline content, as a function of culture time. In TGF-β1 and TGF-β1/IGF-I treated groups, hydroxyproline accumulation showed significant increase over time points ($p<0.001$). Values are mean ± SD ($n=6$). Data were analyzed using two-way ANOVA.

NIH-PA Author Manuscript
NIH-PA Author Manuscript
NIH-PA Author Manuscript

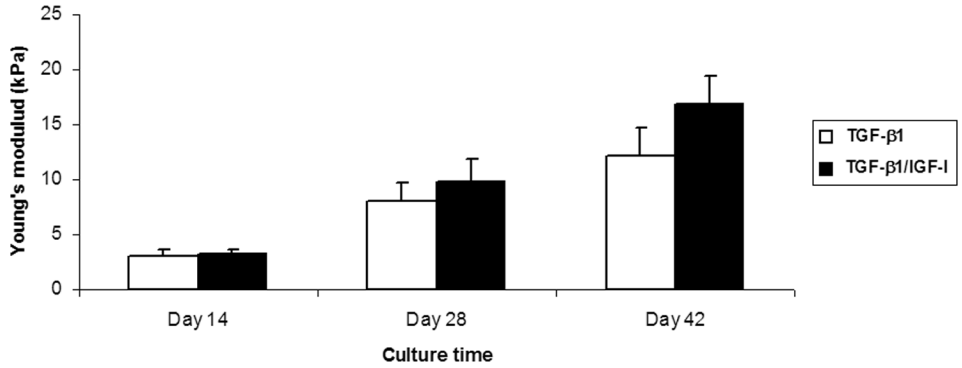

Figure 8.

Mechanical properties of engineered cartilage constructs as a function of culture time. Equilibrium Young's modulus of samples increased with culture time in both growth factor conditions ($p<0.001$). By Day 42, the TGF-β1/IGF-I cultures showed a significant increase compared to TGF-β1 cultures of Day 42 ($p<0.05$). Values are mean ± SD (n=4).

NIH-PA Author Manuscript
NIH-PA Author Manuscript
NIH-PA Author Manuscript

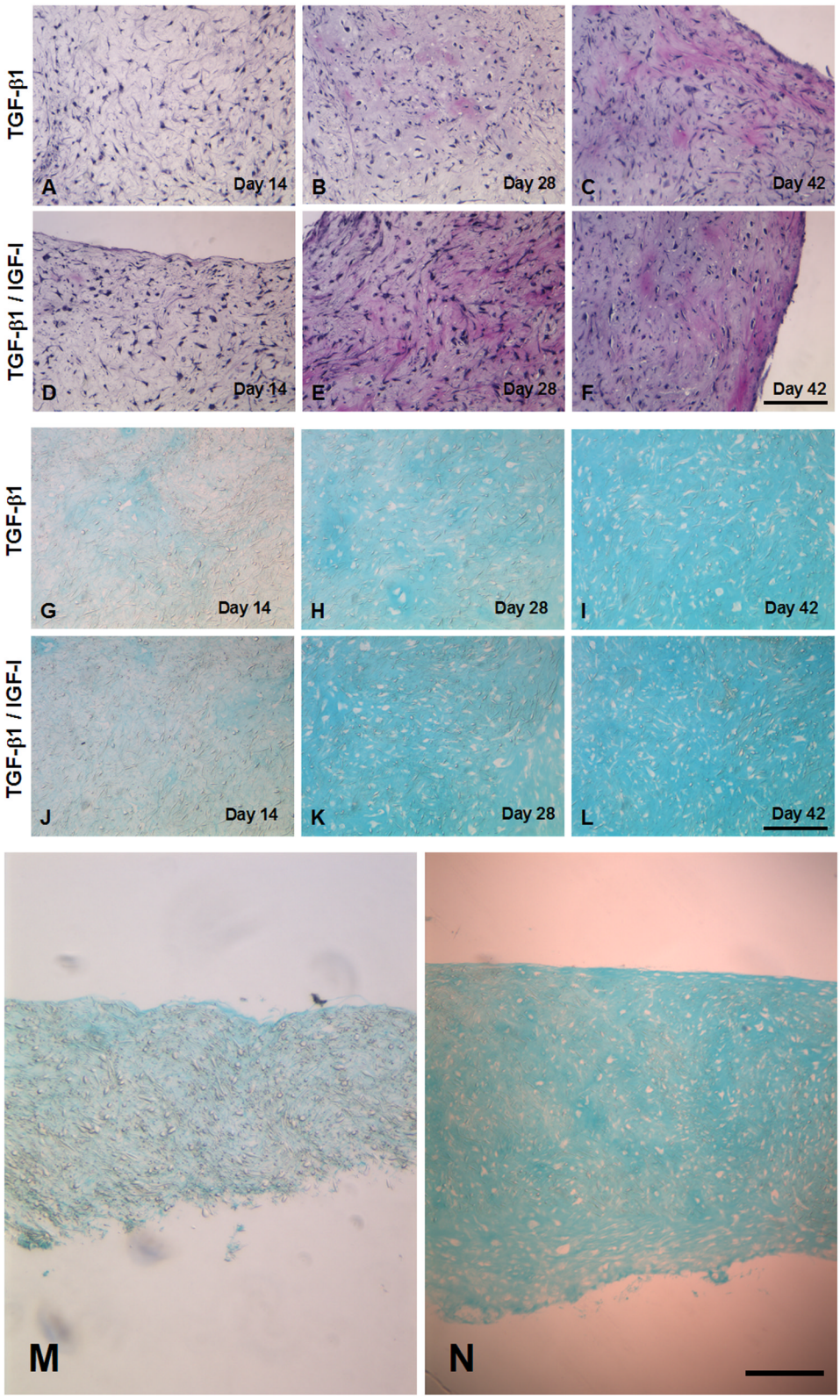

Figure 9.

NIH-PA Author Manuscript

NIH-PA Author Manuscript

NIH-PA Author Manuscript

Histology of engineered cartilage constructs as a function of culture time. Both TGF-β1 and TGF-β1/IGF-I cultures display similar histology. **(A–F) H&E staining**. Regions of varying cell density are seen in early cultures (A, D: Day 14, and B, E: Day 28). A more uniform cell density is seen on Day 42 (C, F). Total cell number remains unchanged, as indicated by constant DNA content (see Figure 5). Bar = 100 μm. **(G–N) Alcian blue staining**. (G–L) High magnification showing increased Alcian blue staining as a function of culture time. Weak staining is seen on Day 14 (G, J). Cells become surrounded by sulfated proteoglycan-rich matrix beginning on Day 28 (H, K). By Day 42, samples from both medium conditions demonstrated extensive accumulation of sulfated proteoglycan-rich ECM. Bar = 100 μm. (M, N) Low magnification view of Day 28 constructs illustrating regional difference in staining intensity. Increased staining is seen at the edges (N), as compared to sections through the middle of the constructs (M). This pattern is not observed in Day 14 TGF-β1/IGF-I constructs (not shown). Bar = 500 μm.